In situ reflection–absorption infrared spectroscopy at the liquid–solid interface: decomposition of organic molecules on polycrystalline platinum substrates

Zhen Ma and Francisco Zaera*

Department of Chemistry, University of California, Riverside, CA 92521, USA

Received 10 February 2004; accepted 21 April 2004

The room-temperature adsorption and surface chemistry of several categories of organic molecules used as reactants or solvents in liquid-phase catalysis, of carboxylic acids, esters, aldehydes, acetone, alcohols and ethers in particular, were characterized *in situ* on polycrystalline Pt in the presence of the liquid phase by reflection-absorption infrared spectroscopy (RAIRS). For carboxylic acids and esters it was found that the propensity for decomposition and CO formation follows a formic acid $\gg$ methyl formate, ethyl formate $>$ acetic acid, propionic acid, acrylic acid, ethyl acetate sequence. For aldehydes and acetone, the observed trend is formaldehyde $\gg$ acetaldehyde $>$ acrolein, crotonaldehyde $>$ propionaldehyde, acetone. Virtually no adsorbed CO was detected when Pt surfaces were exposed to liquid solutions of either alcohols or ethers. The observed trends could be correlated with the corresponding molecular structures. They are discussed in the context of previous results obtained from studies under ultrahigh vacuum (UHV) and under electro-oxidation conditions.

KEY WORDS: liquid–phase catalysis; dissociative adsorption; carbon monoxide; platinum; reflection-absorption infrared spectroscopy; liquid–solid interface.

1. Introduction

In most heterogeneous catalytic processes, the catalysts are solids and the reactants are present in either gas or liquid phases. Compared with the gas–solid counterpart, liquid–solid heterogeneous catalysis offers some attractive features, including mild reaction conditions, narrow product distributions, and better suitability for the production of large pharmaceutical or fine chemicals. Much effort has been devoted to the development of liquid–phase heterogeneous catalysis for selective oxidations [1,2], photochemistry [3], hydrogenations [4], enantioselective synthesis [5] and acid-base reactions [6,7], among others, but less work has been carried out on the elucidation of the molecular aspects of this catalysis [8,9]. *In situ* characterization methods, in particular optical spectroscopies such as sum frequency generation (SFG) [10], infrared spectroscopy (IR) [11–13], and surface-enhanced Raman spectroscopy (SERS) [14,15] promise to play an important role in this endeavor.

We in our laboratory have been using reflection–absorption infrared spectroscopy (RAIRS) both under ultrahigh vacuum (UHV) [12,16,17] and in liquid–solid interfaces [18–21] to extract fundamental information on the surface chemistry of catalysis. In particular, the adsorption of cinchona alkaloids from CCl_4 solutions onto polycrystalline Pt surfaces has been studied recently with the aid of a special liquid cell for *in situ* RAIRS studies [18–21]. The adsorption of these chiral cinchona alkaloids is of great interest because they can act as modifiers to impart chirality to Pt catalysts for the enantioselective hydrogenation of α-ketoesters [5]. Our studies on the adsorption of cinchona from solutions have demonstrated the applicability of *in situ* RAIRS to probe catalytic liquid–solid interfaces, and have provided some insights on the role of both adsorption geometry and the nature of the solvent and dissolved gases into defining the enantioselectivity of this catalysis [18–21]. In this report, another case study of liquid–solid interfacial chemistry, the adsorption and decomposition of simple organic molecules on polycrystalline Pt surfaces under realistic conditions, is presented.

Understanding the chemistry of common organic reactants or solvents on catalytic surfaces is key to the development of catalytic processes. In particular, some solvents may react on the surface of the catalyst to form CO or other potentially poisoning byproducts. Adsorbed CO is known to retard, or even completely inhibit, reactions such as olefin hydrogenation [22,23], fuel cell conversion [24], and enantioselective hydrogenation [25]. Vibrational spectroscopy, in conjunction with temperature-programmed desorption (TPD), cyclic voltammetry (CV), and other surface-sensitive techniques, have been used to develop detailed mechanisms on the decomposition of many organic molecules on metal single crystals in both UHV and electrochemical settings [26–35]. However, extrapolation of the results from these studies

*To whom correspondence should be addressed.
E-mail: francisco.zaera@ucr.edu

1011-372X/04/0700–0005/0 © 2004 Plenum Publishing Corporation

to liquid-phase heterogeneous catalysis is not always straightforward. Therefore, to probe the possibility of CO formation during liquid-phase catalysis, especially during liquid-phase hydrogenations with transition metals such as Pt where the performance of catalysts is quite sensitive to any CO adsorption [23,25], *in situ* characterization under conditions similar to those of the working catalysts is highly desirable.

In this work, the possible room-temperature decomposition of several categories of organic molecules, including carboxylic acids, esters, aldehydes, acetone, alcohols, and ethers, to adsorbed CO on liquid–Pt interfaces in the presence of H_2 is surveyed. *In situ* liquid–solid RAIRS data were obtained as a function of the concentration of the organic solutions, and the ease of CO formation from these reactants and solvents was probed as a function of molecular structure.

2. Experimental

The *in situ* RAIRS experiments reported here were conducted in a homemade liquid–solid RAIRS cell designed for single-reflection IR experiments using a Mattson Sirius 100 FTIR spectrometer. A picture of the optical arrangement used in the IR compartment is provided in figure 1. The IR beam that emerges from the interferometer of the FTIR instrument is first passed through a linear polarizer, mounted on a rotational stage for the selection of s- or p-polarized light. That beam is then focused through a transparent CaF_2 prism onto a polished polycrystalline Pt disk with mirror-like finish, and the reflected light collected and refocused into a mercury–cadmium–telluride (MCT) detector. The liquid solution is trapped between the Pt disk and the CaF_2 prism used to let the IR beam in and out of the cell. More details on this setup are reported elsewhere [19]. Similar arrangements are common in electrochemical studies [34], and have proven quite useful for the *in situ* characterization of liquid–metal interfaces.

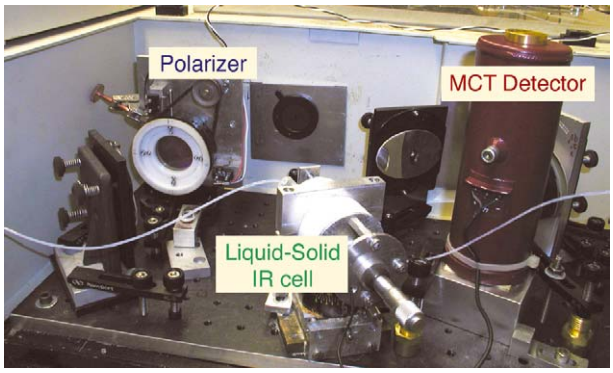

Figure 1. Photograph of the optical arrangement in the *in situ* liquid–solid RAIRS setup used in these experiments. The IR beam exits a commercial Mattson FTIR spectrometer through a port located in the left-hand side of the picture, and is made to travel to an MCT detector by sequentially passing it through a linear polarizer, a parabolic focusing mirror, the CaF_2 prism and polished Pt surface of the liquid–solid IR cell, a collimating mirror, and a final focusing mirror. Additional arrangements are made for gas and liquid sample introduction and for the electronics used to pretreat the Pt disk, as described in more detail elsewhere [19,20].

The Pt sample was cleaned before each experiment by electrochemical oxidation-reduction cycles (ORCs) in 0.1 M $KClO_4$ for 1 h. The electrolyte was then displaced by water, the Pt sample pressed tightly against the prism to form a thin liquid film, and two reference IR spectra recorded, with p- and s-polarized light respectively. The Pt disk was pulled back, the water displaced by the organic solution to be studied, and H_2 bubbled through the liquid at a rate of 0.85 cm^3/min for 0.5 h to maintain the reduced state of the Pt surface [20]. Finally, the Pt disk was again pressed against the prism, and new p- and s-polarized spectra were recorded. The resulting p/s ratio traces were divided by the equivalent background p/s data obtained with the water film. All the reported spectra correspond to averages from 512 scans, taken with 4 cm^{-1} resolution. All the experiments were carried out at ambient temperature (295 ± 2 K).

Formic acid (EM, 98 + %), formic-^{13}C acid (99 atom% ^{13}C), acetic acid (99.99 + %), propionic acid (99.5 + %), acrylic acid (99%), methyl formate (99%), ethyl formate (97%), ethyl acetate (99.5 + %), formaldehyde (37 wt% aqueous solution), formaldehyde-^{13}C (99 atom% ^{13}C, 20 wt% aqueous solution), acetaldehyde (99.5 + %), propinaldehyde (97%), acrolein (Afla Aesar, 97%), crotonaldehyde (99 + %), acetone (99.9 + %), methanol (99.9%), ethanol (99.5 + %), 1-propanol (99.7%), iso-propanol (99.5%), 1-butanol (Fisher, 99.8%), ethyl ether (EM, 99 + %), and isopropyl ether (99%) were all purchased from Aldrich unless otherwise indicated, and used as obtained. MilliQ water was used to prepare the $KClO_4$ electrolyte solutions, and distilled water was used to prepare the aqueous solutions of the organic compounds. H_2 (Liquid Carbonic, 99.999%) CO (Matheson, 99.5 + %), ^{13}CO (Matheson, 99 + %), and O_2 (Matheson, 99.99%) were used as supplied.

3. Results

3.1. Carboxylic acids and esters

In situ RAIRS spectra recorded after exposure of the Pt surface to aqueous formic acid (HCOOH) solutions of various concentrations are displayed in figure 2. In this and all following figures, most traces correspond to the results from independent experiments starting with clean platinum, except for those where a surface initially exposed to the organic solution is subsequently flushed with pure water (the bottom trace in this case). Clear decomposition of the formic acid to carbon

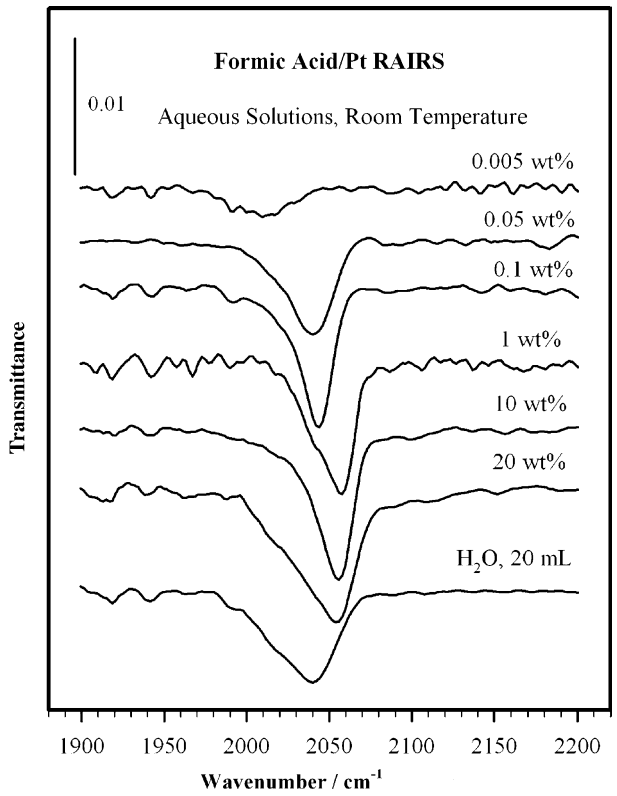

Figure 2. RAIRS data summarizing the surface chemistry of aqueous formic acid solutions on polycrystalline Pt at room temperature. Shown are spectra obtained for the resulting adsorbed carbon monoxide as a function of the concentration of the formic acid. Appreciable CO formation is seen for concentrations as low as 0.005 wt%, and CO coverages close to saturation are reached with concentrations above 1 wt%. The resulting high-coverage CO layer is not readily removed by water flushing.

monoxide is evident in all the cases reported in figure 2. Even for concentrations as low as 0.005 wt% (ca. 0.001 M) of formic acid, a peak at 2010 cm^{-1} corresponding to the C–O stretching frequency of the resulting CO adsorbed on the platinum surface is still appreciable. A CO coverage close to saturation is obtained with a 1 wt% concentration solution, and no obvious increase is seen with more concentrated solutions. The CO coverage obtained with the 20 wt% formic acid solution decreases somewhat after flushing the cell with 20 mL of water, as indicated by a weaker CO peak, also red-shifted from 2054 to 2040 cm^{-1}, seen in the bottom trace of figure 2. Further water treatments do eventually remove all of the adsorbed CO from the surface (data not shown), probably because of surface oxidation by oxygen from air dissolved in the water [13,20]. The formation of adsorbed CO from aqueous formic acid, as seen here, may explain a previous finding that the addition of small amounts of formic acid decreases the rate of liquid-phase hydrogenation of ethyl pyruvate on Pt catalysts [36]: the resulting CO on the Pt surface is likely to block ethyl pyruvate adsorption sites.

It is worth mentioning that the peak positions for the high-coverage CO in figure 2 are slightly lower than those of saturated CO at the H_2O/Pt and CCl_4/Pt interfaces (2054–2058 vs. 2059–2067 and 2074–2080 cm^{-1}) [19,20]. This difference may be explained not only by the H_2 treatment used in our experiments after the introduction of formic acid solutions (the co-adsorption of H_2 on Pt causes a red shift of the CO peak [11,20,37]), but also by the lower surface coverage of CO resulting from the deposition of other species from decomposition of the organic molecules. Unfortunately, the identification of these surface moieties was not possible in our experiments because of the strong IR absorption of the liquid-phase species, the signals of which do not completely cancel out by ratioing p/s spectra [13,34]. Also to note is the absence of detectable signals for bridged-adsorbed CO around 1800–1860 cm^{-1} (not shown). In fact, on Pt, the bridged-adsorbed CO peaks are always much weaker than the linearly adsorbed CO peaks at 2000–2100 cm^{-1} [11,13,34]. In addition, IR absorption by water vapor in the path of the beam interferes with the observation of that inherently weak peak [38], and therefore the absence of detectable features below 1900 cm^{-1} does not provide a clear indication of the absence of multiply coordinated surface CO.

In contrast with the case of formic acid, virtually no adsorbed CO is detected when the Pt surface is exposed to acetic acid (CH_3COOH), propionic acid (C_2H_5COOH), or acrylic acid (CH_2=$CHCOOH$); the decomposition of those longer-chain carboxylic acids on Pt is not apparent under our experimental conditions. In terms of the surface chemistry of esters, figure 3 summarizes the infrared spectroscopy results obtained for neat methyl formate ($HCOOCH_3$), ethyl formate ($HCOOC_2H_5$), and ethyl acetate ($CH_3COOC_2H_5$). When the Pt surface is exposed to methyl formate, two clear and strong bands are seen in the reported wavenumber region at 2069 and 2133 cm^{-1}. They are ascribed to the liquid methyl formate film trapped above the Pt surface; their positions and relative intensities referred to the other bands of methyl formate agree well with standard IR data [39]. In addition, a small CO feature centered at 2004 cm^{-1} is also detected. After replacing the methyl formate with 20 mL of water, the bands due to methyl formate disappear, but the CO peak remains, albeit blue-shifted to 2027 cm^{-1}. Similar formation of adsorbed CO is seen when Pt is exposed to ethyl formate, but not to ethyl acetate. For the latter case, the infrared bands seen at 1892, 2013 and 2089 cm^{-1} in the presence of the organic liquid are assigned to the ethyl acetate itself [40], while the additional small features observed below 2000 cm^{-1} are due to water vapor in the path of the IR beam [19,34]. In summary, methyl formate and ethyl formate do decompose to form CO on Pt, but their conversion is not as facile as that of formic acid.

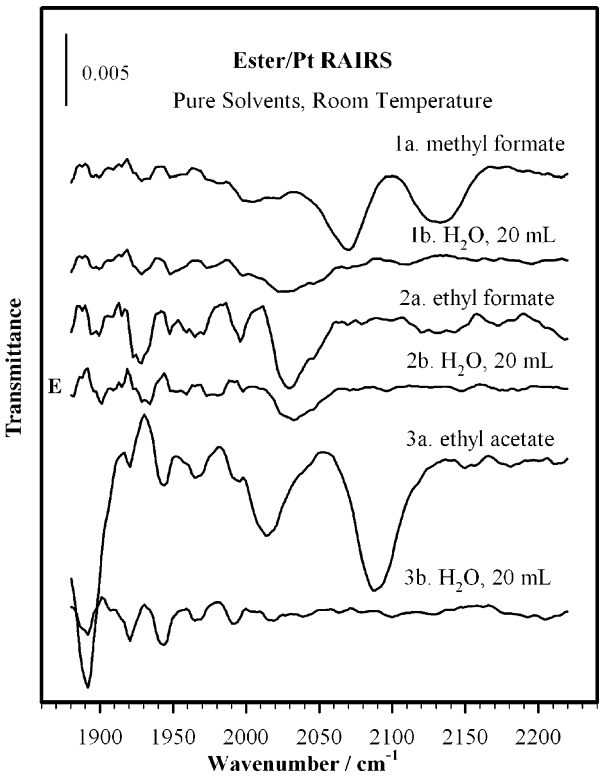

Figure 3. RAIRS data to probe the possible formation of adsorbed CO from several liquid esters. The main spectral features seen during exposure of the Pt surface to the neat esters (traces 1a, 2a, and 3a) are ascribed to the liquid-phase molecules, and disappear after the liquids are flushed with water (traces 1b, 2b, and 3b). Nevertheless, small peaks at 2027 and 2033 cm^{-1} due to adsorbed CO are still observable in the cases of methyl and ethyl formates, respectively. No evidence for the formation of adsorbed CO from ethyl acetate was obtained.

3.2. Aldehydes and acetone

The IR results obtained after exposing Pt surfaces to formaldehyde (HCHO) solutions are collected in figure 4a. Even for concentration as low as 0.01 wt% (ca. 0.003 M), a peak corresponding to linearly bound CO is detected at 2017 cm^{-1}, indicating that the decomposition of formaldehyde to carbon monoxide on Pt is quite facile even at room temperature. The resulting CO IR peak gradually increases in intensity, and blue shifts with increasing concentration up to 5 wt%, at which point the surface coverage of CO is slightly below saturation. The area of the IR peak corresponding to adsorbed CO decreases by about 15% after the 37 wt% solution is flushed once with 20 mL of water, while its position shifts from 2052 to 2044 cm^{-1}. This CO peak almost completely disappears from the IR spectra after a second water rinsing (data not shown).

The formation of adsorbed CO from acetaldehyde (CH_3CHO) on Pt surfaces was studied next. As seen in figure 4b, no adsorbed CO is observable when Pt is exposed to a 0.05 wt% aqueous acetaldehyde solution, but some CO is detected when the concentration reaches 1 wt% (ca. 0.2 M). The CO coverage on the surface increases with acetaldehyde concentration, but the yield of adsorbed CO is much lower than those obtained with formaldehyde (figure 4a): the CO coverage derived from a 40 wt% acetaldehyde solution is comparable to that obtained with a formaldehyde solution with concentration as low as 1 wt%. The CO IR peak from acetaldehyde decomposition, centered at 2031 cm^{-1}, decreases to some extent and blue-shifts reproducibly to 2040 cm^{-1} after the 40 wt% solution is displaced by 20 mL of water.

The adsorption of propionaldehyde (C_2H_5CHO), acrolein (CH_2=CHCHO) and crotonaldehyde (CH_3 CH=CHCHO) on Pt was probed as well. Because these long-chain aldehydes are almost immiscible with water and also have high volatilities and strong smells, 20 wt% alcoholic (instead of aqueous) solutions were used. As summarized in figure 5, a common band at 1924 cm^{-1} is seen for all those solutions. This band is assigned here to the liquid ethanol solvent based on the following facts: (1) A similar peak is seen in the IR spectra of gaseous and liquid ethanol in the absence of Pt [39,40] as well as in our blank tests with pure ethanol; (2) large intensities for that peak are seen in both spectra recorded with p- and s-polarized light; (3) the band intensity of this feature varies proportionally with those of other ethanol bands when the thickness of the liquid film is varied; and (4) this band disappears after the alcoholic solutions are displaced by water. Aside from the 1924 cm^{-1} band ascribed to ethanol, some additional small features assignable to the aldehydes are also observed in the 2050–2200 cm^{-1} range in figure 5. Peaks centered at 2017 and 2015 cm^{-1} are observed when Pt surfaces are exposed to acrolein and crotonaldehyde solutions, respectively. Those CO peaks remain after water flushing, even if blue-shifted to 2031 cm^{-1}. The formation of adsorbed CO from both acrolein and crotonaldehyde on Pt(111) around room temperature has been previously reported under UHV conditions [29,30]. In fact, the deactivation of the catalyst during the liquid-phase hydrogenation of crotonaldehyde on Pt/SiO_2 has been ascribed to the formation of adsorbed CO [41]. In the case of propionaldehyde, no CO peak is detected initially in our IR experiments, but a small feature centered at 2017 cm^{-1} is marginally detected after water flushing. Nevertheless, the final CO coverage is much lower than that originated from either formaldehyde or acetaldehyde (figure 4).

In our prsent study, no adsorbed CO from the decomposition of acetone (CH_3COCH_3) was detected on Pt at ambient temperature either before or after acetone displacement by water, indicating that the reactivity of that organic, a constitutional isomer of propionaldehyde, is much lower than that of formaldehyde. Acetone decomposition to CO on a Pt foil under UHV has been reported to start about room temperature, but to peak around 433 K [42].

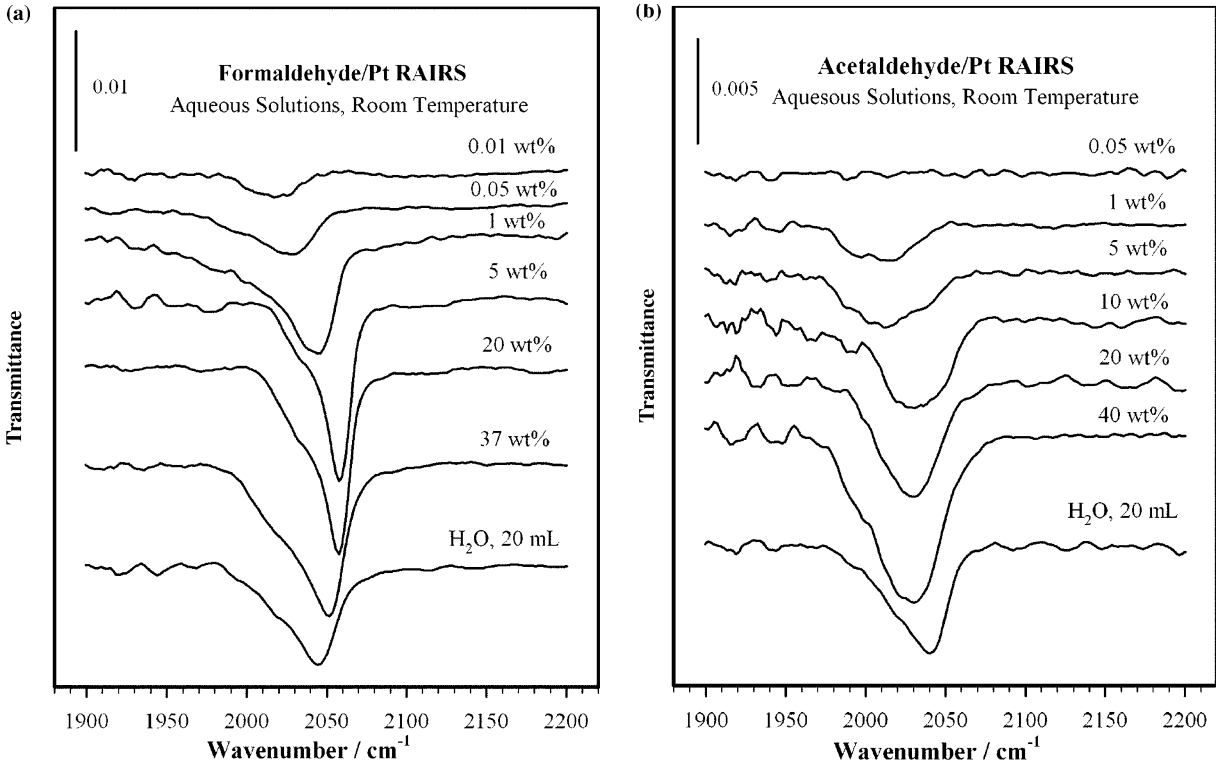

Figure 4. RAIRS data for the formation of adsorbed CO from aqueous solutions of formaldehyde (a, left) and acetaldehyde (b, right) as a function of concentration. CO formation is facile with formaldehyde, where CO saturation is reached on the Pt surface with concentrations as low as 5 wt%. High, although lower, reactivity is observed with acetaldehyde. The high coverage of CO produced by the decomposition of these aldehydes survives a subsequent flushing treatment with water.

3.3. Alcohols and ethers

Figure 6a displays IR data obtained after exposing Pt to methanol (CH_3OH) solutions. No CO peak is detected for concentrations below 5 wt%, but a band develops at 2021 cm^{-1} when the concentration reaches 20 wt%, and keeps on growing and shifts to 2038 and 2046 cm^{-1} for 80 wt% and pure methanol, respectively. However, although that feature appears in the wavenumber region typically associated with linearly bound CO, it nevertheless seems not to correspond to adsorbed CO, but to be associated with the liquid methanol instead. Several reasons can be provided for this conclusion: (1) a small but distinct peak is unambiguously seen in this region in IR spectra of gaseous and liquid methanol [39,40]; (2) the intensity of the peak seen in the methanol/Pt system varies proportionally with other methanol bands, and disappears after water flushing (at least some adsorbed CO usually remains after such treatments, see figures 2–5); (3) the peak in the trace for 80 wt% methanol is almost twice as intense as that of a saturated CO monolayer on the Pt surface, and is centered at 2038 cm^{-1} instead of ca. 2060 cm^{-1}; (4) comparable 2038 cm^{-1} bands are seen in the spectra taken with both p- and s-polarized light; and (5) the intensity of this band changes with film thickness (the distance between Pt surface and prism). Results from additional experiments designed to further check this assignment are reported in figure 6b. The first two traces at the top of that figure corroborate that when Pt is exposed to methanol, a big band at 2046 cm^{-1} appears both in the absence and in the presence of H_2. Thereafter, when CO is bubbled into methanol, an additional peak develops at 2062 cm^{-1}; the difference of the traces obtained after minus before introduction of the CO highlights the feature due to CO adsorption after the CO input. After flushing this cell with 20 mL of water, the methanol band at 2046 cm^{-1} is almost totally removed, while the peak associated with the adsorbed CO still remains. Finally, additional water removes that CO as well. These experiments not only put in evidence the potential problems associated with *in situ* studies of liquid–solid interfaces such as this, but also show that methanol does not readily form CO on Pt surfaces under our experimental conditions, a result that contrasts past electrochemical work [33]. It is also worth pointing out that, under UHV, methanol begins to decompose to CO on Pt(111) and Pt (110) single-crystal surfaces at temperature as low as ~200 K [33,43].

Additional experiments were performed with ethanol (C_2H_5OH), 1-propanol (C_3H_7OH), iso-propanol

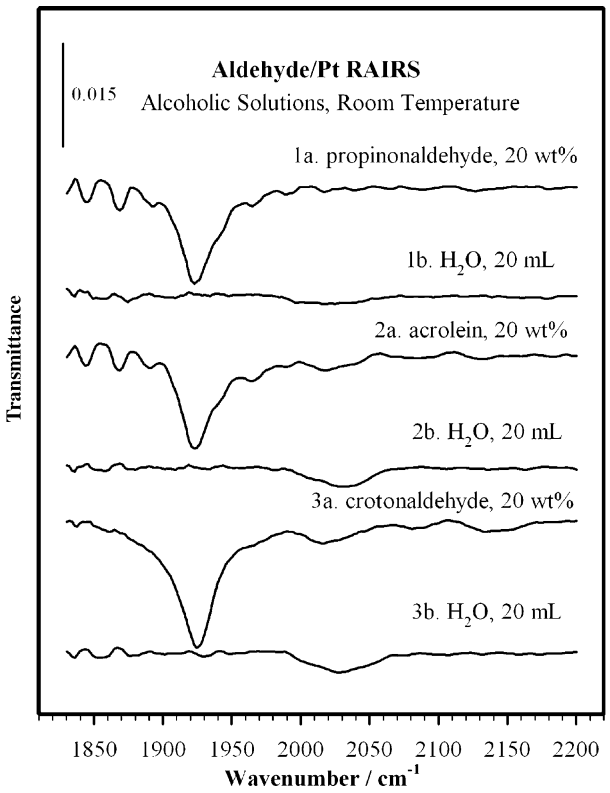

Figure 5. RAIRS results from Pt surfaces, both after exposure to propionaldehyde, acrolein or crotonaldehyde dissolved in ethanol, and after flushing those systems with water. Adsorbed CO from acrolein or crotonaldehyde decomposition is detected by the weak features above 2000 cm^{-1} which become clearer after flushing with water. The formation of adsorbed CO from propionaldehyde, on the other hand, is not apparent in these experiments. The large peak at 1924 cm^{-1} is due to the ethanol solvent.

$[CH_3CH(OH)CH_3]$, 1-butanol (C_4H_9OH), ethyl ether ($C_2H_5OC_2H_5$) and isopropyl ether $[(CH_3)_2CHOCH(CH_3)_2]$. Virtually no CO was detected on those cases in the presence of bubbling H_2 or O_2. For the case of ethanol, a rather faint CO peak appears with concentrations as low as 0.1 wt%, but the CO surface coverage in that case never reaches values higher than 3% of saturation.

3.4. Isotope labeling

Finally, a few additional experiments were performed using selected isotope-labeled molecules to corroborate that the CO detected in our previous experiments does originate from the decomposition of the organics used. For reference, spectra for saturation coverages of ^{12}CO and ^{13}CO on Pt were first obtained by bubbling each of those gases through the IR cell filled with H_2-saturated water. As shown by the top two traces of figure 7, IR peaks develop at 2064 and 2013 cm^{-1} for ^{12}CO and ^{13}CO, respectively, both of similar integrated intensities (corresponding to similar saturation coverages). It is worth noticing that the experimental value obtained with ^{13}CO is quite close to that expected using a simple harmonic oscillator model (2018 cm^{-1}) [44].

The decomposition of 1 wt% formic-^{13}C acid was tested next. A weak ^{13}CO peak appears in that case at ~1965 cm^{-1} (figure 7, third trace from the bottom), a value that should correspond to a vibration at 2012 cm^{-1} if ^{12}CO were produced from formic-^{12}C acid instead. However, the experimental value measured with a 1 wt% formic-^{12}C acid solution is 2057 cm^{-1} instead (figure 7, third trace from the top). In view of the intensity and position of the resulting ^{13}CO peak in these experiments, it's clear that the surface coverage of ^{13}CO is significantly lower than saturation. This suggests that the propensity of the adsorbed formic-^{13}C acid towards decomposition may be lower than that of the regular formic-^{12}C acid [45]. Alternatively, these results could be a reflection of small changes in adsorption coverages due to the presence of contaminants in the formic-^{13}C acid solution, or, perhaps more likely, to isotopic dilution in the case of the ^{13}C-labeled compound. Nevertheless, it is clear that the general conclusion that the adsorbed CO seen by IR originates from the decomposition of the adsorbed organic molecules still holds true.

A similar shift in C–O vibration is observed for the case of a 1 wt% formaldehyde-^{13}C solution, where a ^{13}CO peak is observed at 1984 cm^{-1} (figure 7, bottom trace). Again, while the corresponding peak for ^{12}CO from formaldehyde-^{12}C would be expected at 2029 cm^{-1}, a ^{12}CO signal at 2044 cm^{-1} was observed experimentally instead (figure 7, second trace from the bottom). However, in this case the frequencies and the integrated IR signals for the ^{12}CO and ^{13}CO are both much closer to the expected values (the signal for ^{13}CO being only about 15% smaller than that for ^{12}CO), suggesting closer final CO coverages with both isotopes.

4. Discussion and conclusions

As mentioned in the Introduction, some organic molecules, including many liquid reactants and solvents commonly used in catalysis, may decompose on solid surfaces to form other adsorbed species. UHV studies have furnished detailed mechanisms for these reactions at vacuum–solid interfaces, but extrapolation of those results to liquid–phase heterogeneous catalysis is not always straightforward. Electrochemical studies have added to our understanding of liquid–solid interfaces, but the presence of both electrochemical potentials and strong electrolytes, as well as the rather low concentration of organic molecules often used in those systems, confine the scope of their applications. In order to determine the potential effect of liquid decomposition in heterogeneous catalysis, *in situ* characterization of

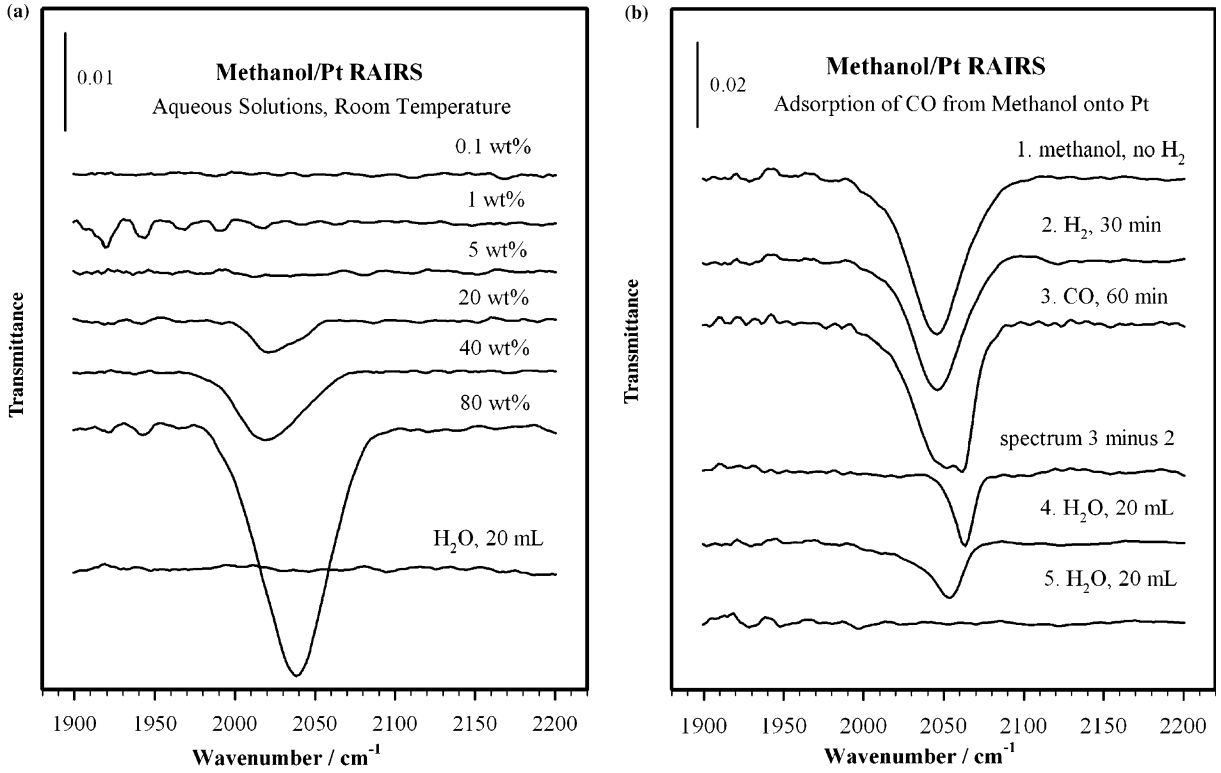

Figure 6. RAIRS results to probe the possible decomposition of methanol on Pt surfaces. The main bands seen in (a) increase with methanol concentration in aqueous solution, and are ascribed to the methanol trapped in the liquid film between the Pt and prism surface; they disappear after the methanol solutions are displaced by water (a, bottom trace). No CO from decomposition is seen in these experiments. The ability to detect adsorbed CO in methanol solutions was tested by the sequence of experiments shown in (b), where CO is bubbled through methanol, after which the cell is flushed with water.

liquid–solid interfaces under more realistic conditions is required.

In this report we have provided results from *in situ* RAIRS studies on the room-temperature surface chemistry of some organic molecules on Pt. In particular, the possible decomposition of several categories of organic compounds, including carboxylic acids, esters, aldehydes, acetone, alcohols, and ethers to CO on polycrystalline Pt was tested. Among carboxylic acids and esters, decomposition to adsorbed CO proved quite easy for formic acid, possible with methyl formate and ethyl formate, and fairly slow for acetic acid, propionic acid, acrylic acid, and ethyl acetate. For aldehydes and acetone, CO formation followed a formaldehyde $\gg$ acetaldehyde $>$ acrolein, crotonaldehyde $>$ propionaldehyde, acetone trend. Finally, virtually no adsorbed CO was detected when Pt surfaces were exposed to methanol, ethanol, 1-propanol, iso-propanol, 1-butanol, ethyl ether, and isopropyl ether. Of all the organic solutions probed in this study, only formaldehyde and formic acid decompose to form close-to-saturated CO layers on Pt surfaces.

The marked differences in reactivity reported here seem to be related to the structure of the organic molecules. First, it appears that molecules containing C=O groups (such as aldehydes, carboxylic acids, and esters) are more likely to decompose to adsorbed carbon monoxide than those with C—O single bonds (such as alcohols and ethers). It is reasonable to propose that the C=O group, with its higher bond order than C—O, may be a more direct precursor to the production of adsorbed carbon monoxide [33,46]. This is certainly the case in organometallic systems, where decarbonylation steps are quite facile. Moreover, surface-science studies on adsorbed alcohols have indicated that, after a facile conversion to the corresponding alkoxide, decomposition occurs via β-hydride elimination to form aldehydes or ketones [33,46–50]. It can be inferred from this study that this dehydrogenation may be slower than the subsequent steps which lead to the adsorbed CO, at least under the hydrogen-rich conditions used in liquid-phase catalytic hydrogenations. Note that under vacuum the initial dehydrogenation step is often favored instead [51].

A second generalization arising from this work is that the substituent groups linked to the carbonyl moiety in the organic molecules play an important role in determining the kinetics of surface decomposition to CO. Clearly, molecules with smaller substituents (such as –H and –OH) are easier to decompose. It may very well be that the trends in reactivity reported here are accounted for by steric effects resulting from substitutions around the central carbonyl moiety with alkyl or alkoxide groups.

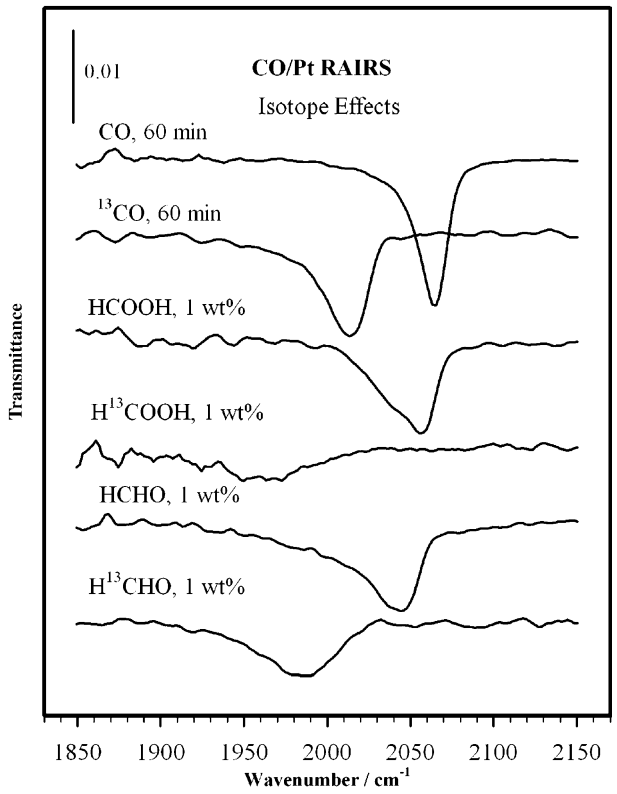

Figure 7. RAIRS data to indicate the kinetic isotope effects associated with the dissociative adsorption of formic acid and formaldehyde liquid solutions on Pt surface. The saturation coverages of ^{12}CO and ^{13}CO were first determined by titration of Pt surfaces with gaseous ^{12}CO and ^{13}CO bubbled through water. Compared with the ^{12}C-containing formic acid and formaldehyde compounds, the ^{13}C-labeled samples manifest lower reactivity. These points to the potential importance of C–H or C–C bond-scission steps in the mechanism of decomposition of these organic compounds.

Acknowledgments

Financial support for this work was provided by grants from the US National Science Foundation and the US Department of Energy.

References

[1] R.A. Sheldon, M. Wallau, I.W.C.E. Arends and U. Schuchardt, Acc. Chem. Res. 31 (1998) 485.
[2] M. Besson and P. Gallezot, Catal. Today 57 (2000) 127.
[3] J.M. Herrmann, Catal. Today 53 (1999) 115.
[4] U.K. Singh and M.A. Vannice, Appl. Catal. A 213 (2001) 1.
[5] A. Baiker and H.U. Blaser, in: *Handbook of Heterogeneous Catalysis,* Vol. 4, eds. G. Ertl, H. Knözinger and J. Weitkamp, (VCH, Weinheim, 1997), p. 2422.
[6] T. Okuhura, Chem. Rev. 102 (2002) 3641.
[7] Y. Ono, J. Catal. 216 (2003) 406.
[8] G.A. Somorjai, Surf. Sci. 335 (1995) 10.
[9] F. Zaera, Surf. Sci. 500 (2002) 947.
[10] G. Rupprechter and G.A. Somorjai, J. Phys. Chem. B 103 (1999) 1623.
[11] D. Ferri, T. Bürgi and A. Baiker, J. Phys. Chem. B 105 (2001) 3187.
[12] F. Zaera, Int. Rev. Phys. Chem. 21 (2002) 433.
[13] I. Ortiz-Hernandez and C.T. Williams, Langmuir 19 (2003) 2956.
[14] W. Chu, R.J. LeBlanc and C.T. Williams, Catal. Commun. 3 (2002) 547.
[15] C. Fokas and V. Deckert, Appl. Spectrosc. 56 (2002) 192.
[16] F. Zaera, in: *Encyclopedia of Chemical Physics and Physical Chemistry*, eds. J. Moore and N. Spencer, (Institute of Physics Publishing, UK, 2001), pp. 1563–1581.
[17] F. Zaera, H. Hoffman and P.R. Griffiths, J. Electron Spectrosc. Relat. Phenon. 54/55 (1990) 705.
[18] J. Kubota and F. Zaera, J. Am. Chem. Soc. 123 (2001) 11115.
[19] J. Kubota Z. Ma and F. Zaera, Langmuir 19 (2003) 3371.
[20] Z. Ma, J. Kubota and F. Zaera, J. Catal. 219 (2003) 404.
[21] Z. Ma, L. Ilkeun, J. Kubota and F. Zaera, J. Mol. Catal. A, in press.
[22] J. Grunes, J. Zhu, M. Yang and G.A. Somorjai, Catal. Lett. 86 (2003) 157.
[23] H. Arnold, F. Döbert and J. Gaube, in: eds. *Handbook of Heterogeneous Catalysis,* Vol. 4, eds. G. Ertl, H. Knözinger and J. Weitkamp, VCH, Weinheim, 1997, p. 2165.
[24] L. Carrette, K.A. Friedrich and U. Stimming, Chem. Phys. Chem 1 (2000) 162.
[25] M. von Arx, T. Mallat and A. Baiker, Top. Catal. 19 (2002) 75.
[26] R.W. McCabe, C.L. DiMaggio and R.J. Madix, J. Phys. Chem. 89 (1985) 854.
[27] T. Ohtani, J. Kubota, A. Wada, J.N. Kondo, K. Domen and C. Hirose, Surf. Sci. 368 (1996) 270.
[28] W.-H. Hung and S.L. Bernasek, Surf. Sci. 346 (1996) 165.
[29] J.C. de Jesús and F. Zaera, J. Mol. Catal. A 138 (1999) 237.
[30] J.C. de Jesús and F. Zaera, Surf. Sci. 430 (1999) 99.
[31] R.D. Haley, M.S. Tikhov and R.M. Lambert, Catal. Lett. 76 (2001) 125.
[32] L.W.H. Leung and M.J. Weaver, J. Phys. Chem. 93 (1989) 7218.
[33] K. Franaszczunk, E. Herrero, P. Zelenay, A. Wieckowski, J. Wang and R.I. Masel, J. Phys. Chem. 96 (1992) 8509.
[34] T. Iwasita and F.C. Nart, Prog. Surf. Sci. 55 (1997) 271.
[35] W.F. Lin and P.A. Christensen, Faraday Discuss. 121 (2002) 267.
[36] H.U. Blaser, H.P. Jalett and J. Wiehl, J. Mol. Catal. 68 (1991) 215.
[37] M. Primet, J.M. Basset, M.V. Mathieu and M. Prettre, J. Catal. 29 (1973) 213.
[38] Y. Ikezawa, H. Saito, H. Matsubayashi and G. Toda, J. Electroanal. Chem. 252 (1988) 385.
[39] Standard IR Data, http://www.sigmaaldrich.com.
[40] Standard IR Data, http://webbook.nist.gov/chemistry.
[41] M. Englisch, V.S. Ranade and J.A. Lercher, Appl. Catal. A 163 (1997) 111.
[42] Z.M. Liu and M.A. Vannice, Surf. Sci. 316 (1994) 337.
[43] B.A. Sexton, K.D. Rendulic and A.E. Hughes, Surf. Sci. 121 (1982) 181.
[44] D.P. Shoemaker, C.W. Garland and J.W. Nibler, *Experiments in Physical Chemistry* 6th edn. (McGraw-Hill, Boston, 1996), p. 400.
[45] K.J. Laidler, *Chemical Kinetics* (Haper Collins Publishers, New York, 1987).
[46] R.I. Masel, *Chemical Kinetics and Catalysis*, (Wiley-Interscience, New York, 2001) p. 284.
[47] M. Mavrikakis and M.A. Barteau, J. Mol. Catal. A 131 (1998) 135.
[48] M.K. Weldon and C.M. Friend, Chem. Rev. 96 (1996) 1391.
[49] N. Gleason, J. Guevremont and F. Zaera, J. Phys. Chem. B 107 (2003) 11133.
[50] F. Zaera, Catal. Lett. 91 (2003) 1.
[51] F. Zaera, Chem. Rev. 95 (1995) 2651.